

Systemically Delivered, Deep-Tissue Nanoscopic Light Sources

Xiang Wu^{1, 2, *}, Fan Yang^{1, 2}, Sa Cai^{1, 2}, and Guosong Hong^{1, 2, *}

Abstract—Light is widely used in life science in both controlling and observing biological processes, yet a long-standing challenge of using light inside the tissue lies in the limited penetration depth of visible light. In the past decade, many *in vivo* light delivery methods using photonics and materials science tools have been developed, with recent demonstrations of non-invasive, deep-tissue light sources based on systemically delivered luminescent nanomaterials. In this perspective, we provide an overview for the principles of intravital nanoscopic light sources and discuss their advantages over existing methods for *in vivo* light delivery. We then highlight their recent applications in optogenetics neuromodulation and fluorescent imaging in live animals. We also present an outlook section about the feasibility of combining these non-invasive light sources with other modalities to expand the utilities of light in biology.

1. INTRODUCTION

Light, especially visible light, has widespread applications in biology, such as fluorescence imaging [1], optogenetics neuromodulation [2], and light-based therapies [3]. However, light is strongly attenuated by biological tissue due to scattering and absorption [1], thus making it challenging to deliver light deep inside the tissue. Although the advances in photonics and materials science have resulted in new modalities for *in vivo* deep-tissue light delivery [4], existing methods usually require the invasive implantation of external devices or injection of nanotransducers [2, 5–7], or have a limited penetration depth up to a few millimeters [8]. Therefore, it is desirable to develop new techniques that can deliver light up to a few centimeters deep inside the tissue without the need for any invasive injection or implantation.

Materials with mechanoluminescence (ML) and persistent luminescence (PerL) have recently emerged as promising candidates to address these challenges [9–13]. Specifically, ML refers to the light emission triggered by mechanical stimuli [14, 15], while PerL refers to prolonged luminescence (from minutes to days) after the cease of photo excitation [16, 17]. Conventional ML and PerL materials are usually micron-sized particles produced by high-temperature solid-state reactions and are mainly used for non-biological applications such as stress sensing for ML materials and decoration and display for PerL materials [14–18]. In the past decade, there has been an increasing research interest in developing nanosized ML and PerL materials for biological applications. Specifically, multiple nanomaterial systems with red or near-infrared (NIR) PerL emissions have been reported for high signal-to-background ratio (SBR) imaging in live animals [19–22], due to the elimination of real-time photoexcitation and thus lower tissue autofluorescence. Although red or NIR photons exhibit reduced scattering inside the tissue and thus allow deeper penetration [6, 23], these long-wavelength photons cannot provide efficient excitation for many biological systems, such as fluorescent proteins [24], light-sensitive ion channels [25], and light-activatable gene-editing tools [26, 27].

To address the energetic challenges with red/NIR emitting materials, new synthesis methods have been developed to yield short-wavelength ML and PerL materials with good water solubility and

Received 27 November 2022, Accepted 14 February 2023, Scheduled 4 April 2023

* Corresponding author: Xiang Wu (xiangwu@stanford.edu), Guosong Hong (guosongh@stanford.edu).

¹ Department of Materials Science and Engineering, Stanford University, Stanford, CA 94305, USA. ² Wu Tsai Neurosciences Institute, Stanford University, Stanford, CA 94305, USA.

sufficient brightness [9–11, 28]. These ML and PerL solutions can be non-invasively delivered through intravenous injection and were used as deep-tissue light sources for various biological applications such as optogenetics neuromodulation and fluorescence imaging in animals. These systemically delivered internal light sources provide many advantages over existing *in vivo* light delivery methods, thus having great potentials to become a versatile platform for extending the capability of optical technologies in biology.

In this perspective, we first present an overview of existing methods for *in vivo* light delivery and discuss their key advantages and constraints. We then highlight the recent demonstrations of circulation-deliverable nanoscopic light sources based on PerL and ML nanomaterials, with an emphasis on their unique advantages over existing methods. Finally, we conclude with an outlook on the potential new possibilities enabled by these emerging internal light sources when they are combined with other light-activatable biological systems. For a more comprehensive review of optical techniques in biology, PerL and ML nanomaterials, we refer the readers to several existing reviews [3, 4, 14–17].

2. IN VIVO LIGHT DELIVERY METHODS

The conventional method for *in vivo* light delivery is to place an external light source outside the tissue (Figure 1(a)), which is commonly used for fluorescence imaging in live animals [1]. This approach can be totally non-invasive and is the preferred method of illumination in the shallow tissue and special organisms such as the transparent zebrafish [29]. However, the strong scattering of light in many mammalian tissues severely perturbs its wavefront, thus confining the effective light delivery region to only superficial tissue and making it difficult to focus light beyond a few scattering mean free paths ($< 30 \mu\text{m}$ for 532-nm light in mouse brain) [8]. In fact, for fluorophores with visible excitation and emission, even the thin skin tissue in mouse strongly attenuates and distorts the light wavefront, thus necessitating the removal of skin for better imaging quality [30]. Although a recent report used external blue light to non-invasively modulate endogenous Ca^{2+} channels up to a depth of 3.4 mm in the mouse brain via an ultra-sensitive optogenetics system [31], this conventional method of light delivery is not generalizable to other systems that require more photons, and is thus not preferred for deep-tissue light delivery.

One approach to overcome the strong scattering of visible light in the tissue is through wavefront shaping using a spatial light modulator (SLM) (Figure 1(b)). Specifically, by generating a “guidestar” deep inside the tissue and measuring its output wavefront, one can “decode” the deterministic scattering events experienced by the emission photons [32, 33]. The SLM can then be used to “encode” the scattering information into the incident light field by modulating its wavefront, thus achieving deep-tissue focusing beyond multiple scattering mean free paths. For example, combined with multi-photon excitation, adaptive optics with wavefront shaping was able to achieve light focusing and neural activity imaging up to a depth > 1 mm in the highly scattering brain tissue of mice [33, 34]. Furthermore, using an ultrasound-mediated guidestar, Ruan et al. recently demonstrated the tight focusing of 532 nm light inside acute brain slices, with a full width at half maximum (FWHM) $< 30 \mu\text{m}$ up to a depth of 2 mm [8]. Apart from deep-tissue focusing, the light delivery using wavefront shaping offers another advantage: the ease of shifting the location of the guidestar and thus the focus of illumination. However, wavefront shaping methods are generally limited by the performance of SLM and the efficiency of the guidestar [8]. Specifically, the rapid dynamics of biological systems require high-frequency update of the incident wavefront modulated by SLM, which usually has an upper modulation frequency limit of tens of Hz when high precision control is needed. Furthermore, when focusing light deeper inside the tissue beyond $1 \sim 2$ mm, it is less efficient to generate a guidestar, while photons from the guidestar are less likely to be detected, making it increasingly difficult to extract the wavefront information. Additionally, fitting multiple devices (e.g., an ultrasound transducer, a digital optical phase conjugation system, and an SLM) needed for wavefront shaping in the limited space near the tissue of interest on live animals is also quite challenging.

Another widely used method for deep-tissue light delivery is the implantation of external devices or the injection of nanotransducers (Figure 1(c)). The implanted devices include waveguides, such as optical fibers [2, 35], and light emitting devices, such as micro-light emitting diodes (μ -LEDs) [5, 7, 36]. For example, standard *in vivo* optogenetics and fiber photometry protocols usually use fiber implants

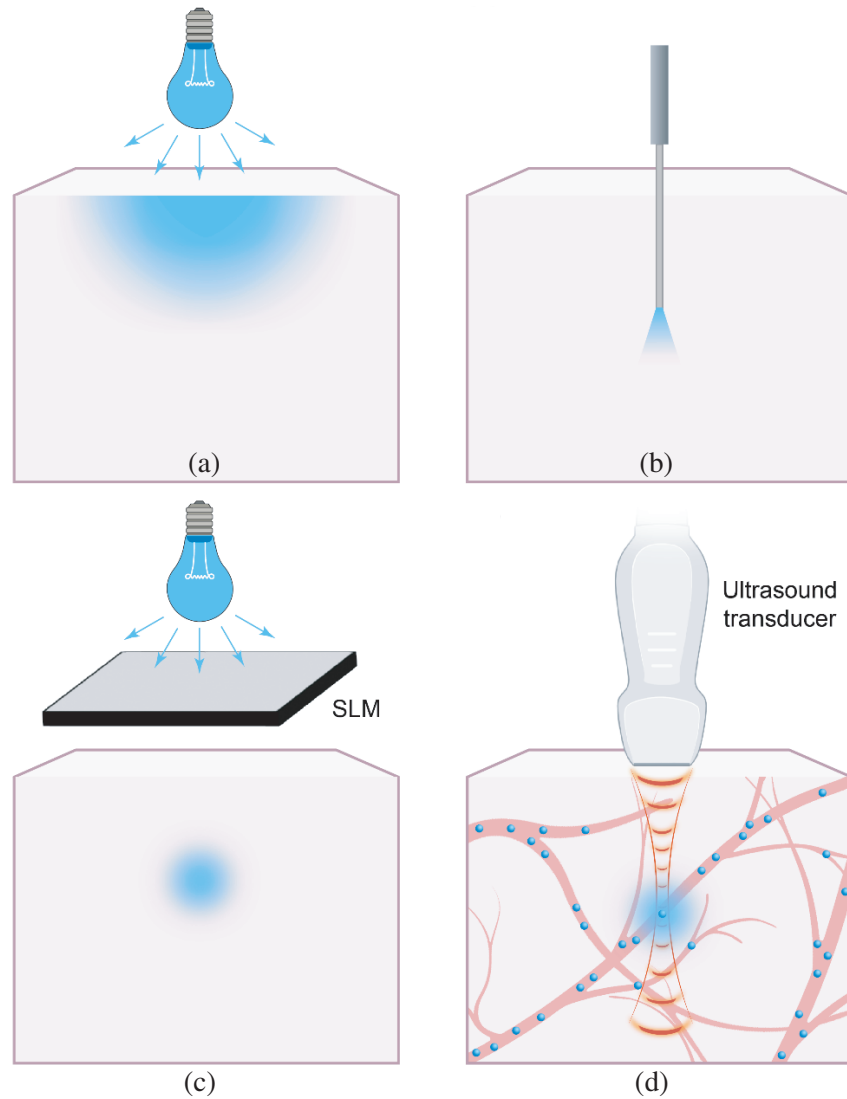


Figure 1. *In vivo* light delivery methods. (a) Conventional external light source [1]. (b) Focused light delivery using wavefront shaping through an SLM [8, 33]. (c) Implanted light source [2, 5, 7, 36]. (d) Ultrasound-mediated internal light source [9, 11, 12].

for deep-brain applications [2, 37], while flexible μ -LEDs also have widespread utilities in both central and peripheral nervous systems [5, 36]. These tissue implants allow efficient local light delivery with almost no constraints on the penetration depth; however, they usually cause acute tissue damage and chronic immune responses around the implantation site [38, 39]. One approach to eliminate chronic tissue responses is through the local injection of nanotransducers that can convert other forms of energy with deeper tissue penetration into visible light [6, 40]. For example, Chen et al. recently used deep-penetrating NIR light to stimulate intracranially delivered upconversion nanoparticles to generate visible light emission for deep-brain optogenetics [6]. The local injection of nanotransducers, however, is still invasive, and the penetration depth of NIR light is usually confined to a few millimeters before the heating on the superficial tissue becomes too significant [23]. Another common challenge associated with all implanted or injected light sources is that the light delivery site cannot be easily relocated. Although fine adjustment of the illumination region near the vicinity of the device has been achieved with tapered fibers or nanophotonic devices [41, 42], it remains challenging to relocate the light delivery site in all three dimensions on the organ level.

3. INTRAVASCULAR LIGHT SOURCES

As summarized in the above section, one key challenge for existing *in vivo* light delivery methods arises from the trade-off between penetration depth and invasiveness: an external light source is non-invasive but only delivers light to the shallow tissue, while an implanted light source provides deep-tissue illumination at the cost of invasiveness. To address this challenge, multiple recent reports have used biocompatible ML and PerL nanomaterials with bright short-wavelength emissions as circulation-deliverable nanoscopic light sources (Figure 1(d)) [9–12]. Specifically, ML materials can produce localized and transient light emission when being stimulated by tissue-penetrant focused ultrasound (FUS). The first example was demonstrated by Wu et al. using ZnS-based blue-emitting

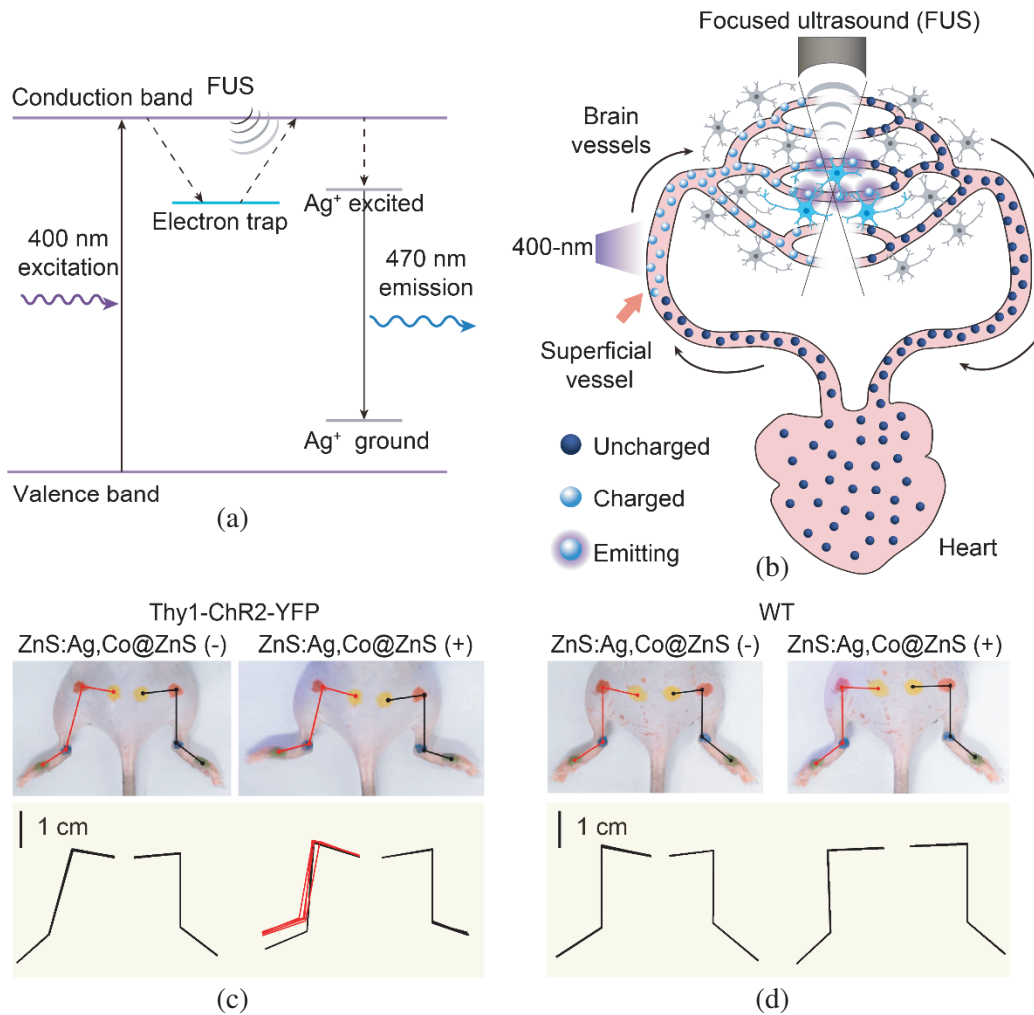


Figure 2. Circulation-delivered internal light sources based on ML nanotransducers. (a) Schematic showing the mechanism of ML from ZnS:Co,Ag. (b) Schematic showing the principle of circulation-delivered internal light sources, where the recharging happens at the superficial vessels, while the discharging is mediated by FUS in the deep tissue. (c), (d) Top: photos of a Thy1-ChR2-YFP mouse (c) and a wildtype (WT) mouse (d) during FUS stimulation before (left) and after (right) ML nanoparticles injection. Bottom: Kinematics of the hindlimb for the two mice in the top panels. The kinematics is the motion induced by motor cortex neural activation as a result of ultrasound-mediated light emission in the brain. The red lines in the bottom right panel of (c) highlight the limb motion induced by ultrasound stimulation. Adapted with permission from [9]. Copyright 2020, American Association for the Advancement of Science.

ML nanotransducers synthesized by a modified sol-gel method [9]. These nanotransducers can store the photoexcitation energy in their trap states created by point defects inside the lattice, before releasing the energy as 470-nm photons upon FUS stimulation which causes trap release (Figure 2(a)). Furthermore, the authors leveraged the endogenous circulatory system to recharge the ML nanotransducers when they pass through superficial blood vessels, thus allowing reproducible ultrasound-mediated light emission inside deep tissue (Figure 2(b)). In another aspect, an *in vivo* “optical flow battery” was created, where the recharging happened in the superficial tissue, and the discharging was mediated by FUS inside deep tissue. As a proof-of-concept demonstration, the authors used this FUS-mediated internal light source for non-invasive optogenetics neuromodulation and observed behavioral responses in live mice (Figures 2(c), (d)), a technique termed “sono-optogenetics” [9].

To expand the ML nanomaterials toolbox for different biological systems, Yang et al. recently reported a biomineral-inspired suppressed dissolution approach to synthesize multi-color ML

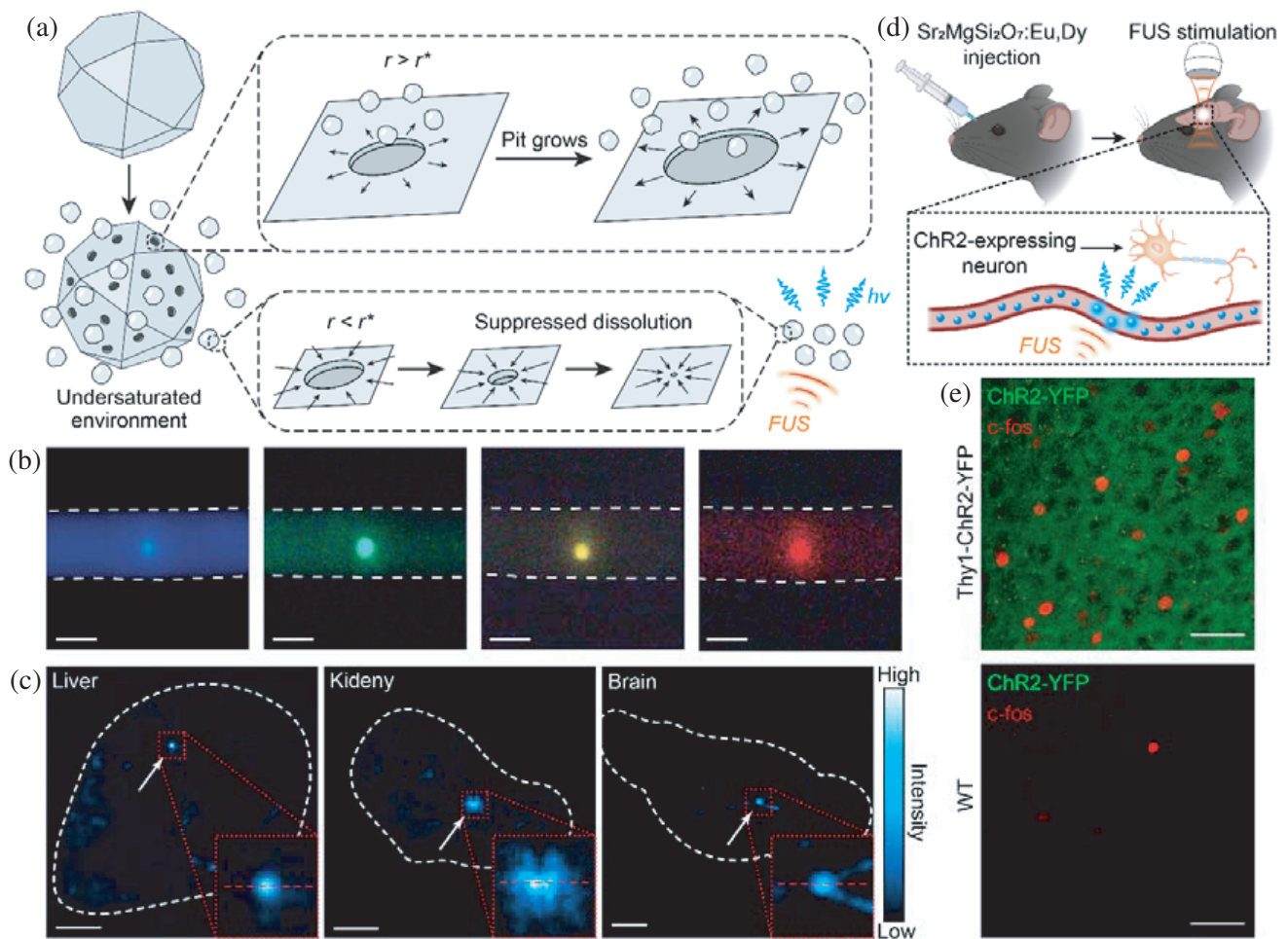


Figure 3. Multicolor internal light sources enabled by ML nanotransducers produced from a biomineral-inspired suppressed dissolution approach. (a) Schematic showing the principle of the biomineral-inspired suppressed dissolution approach. (b) Photos of multicolor ML nanotransducers suspended in aqueous solutions during FUS stimulation. (c) Images of FUS-mediated light emission from multiple mouse organs. (d) Schematic showing the experimental procedures of FUS-mediated non-invasive optogenetic neuromodulation enabled by circulation-delivered ML nanotransducers. (e) Fluorescence imaging of brain slices from a Thy1-ChR2-YFP mouse (top) and a WT mouse (bottom). *c-fos* is an immediate early gene indicating neural activities. The scale bars represent 1 mm in (b), 2 mm in (c) and 40 μm in (e), respectively. Adapted with permission from [11]. Copyright 2022 American Chemical Society.

nanoparticles from their solid-state counterparts (Figure 3) [11]. Specifically, they leveraged a unique phenomenon observed in nature where the dissolution of biominerals is suppressed for nanostructures even in an undersaturated environment (Figure 3(a)). They mimicked this situation using a citrate buffer and produced a palette of ML colloids with emission wavelengths covering the entire visible spectrum (Figure 3(b)). Furthermore, after systemic delivery, the short-wavelength ML nanotransducers could produce localized ($\text{FWHM} \leq 0.5 \text{ mm}$) and transient (on-set response time $\leq 0.5 \text{ ms}$) light emissions inside multiple mice organs upon 1.5-MHz FUS stimulation that penetrated through the entire organ (Figure 3(c)). Importantly, the ML emission was strong enough to activate a light-sensitive ion channel channelrhodopsin-2 (ChR2) inside the mouse brain in a non-invasive manner (Figures 3(d), (e)) [11]. Compared with 470-nm light, which penetrates less than 1 mm inside the biological tissue [1], 1.5-MHz FUS has a tissue penetration depth $> 1 \text{ cm}$ [43]. Another key advantage of the FUS-mediated nanoscopic light sources lies in the ease of relocating the illumination area by simply shifting the ultrasound focus, which is particularly difficult for implanted light sources (Figure 1(c)).

Apart from ML nanomaterials, PerL nanomaterials have also been used as circulation-delivered internal light sources *in vivo*. Similar to ML materials, PerL materials also store photoexcitation energy in the lattice, but gradually emit the energy as light due to the thermal activation. As a result, PerL materials can be used as a continuous light source without the need for real-time in-situ photoexcitation. Specifically, Yang et al. recently synthesized multicolor PerL nanomaterials with exceptional brightness up to $5.25 \times 10^{11} \text{ ps}^{-1} \text{ cm}^{-2} \text{ sr}^{-1}$, which enabled excitation-free brain vascular imaging in live mice (Figures 4(a), (b)) [10]. Furthermore, the blue-emitting PerL nanomaterials acted as an internal light source inside the blood vessels to provide excitation for genetically encoded fluorescent proteins in the mouse brain (Figure 4(c)). Compared with conventional external light sources, this PerL-based internal light source mitigated the challenge of autofluorescence and patterned attenuation from the superficial tissue, thus allowing intracranial fluorescent protein imaging without contamination from

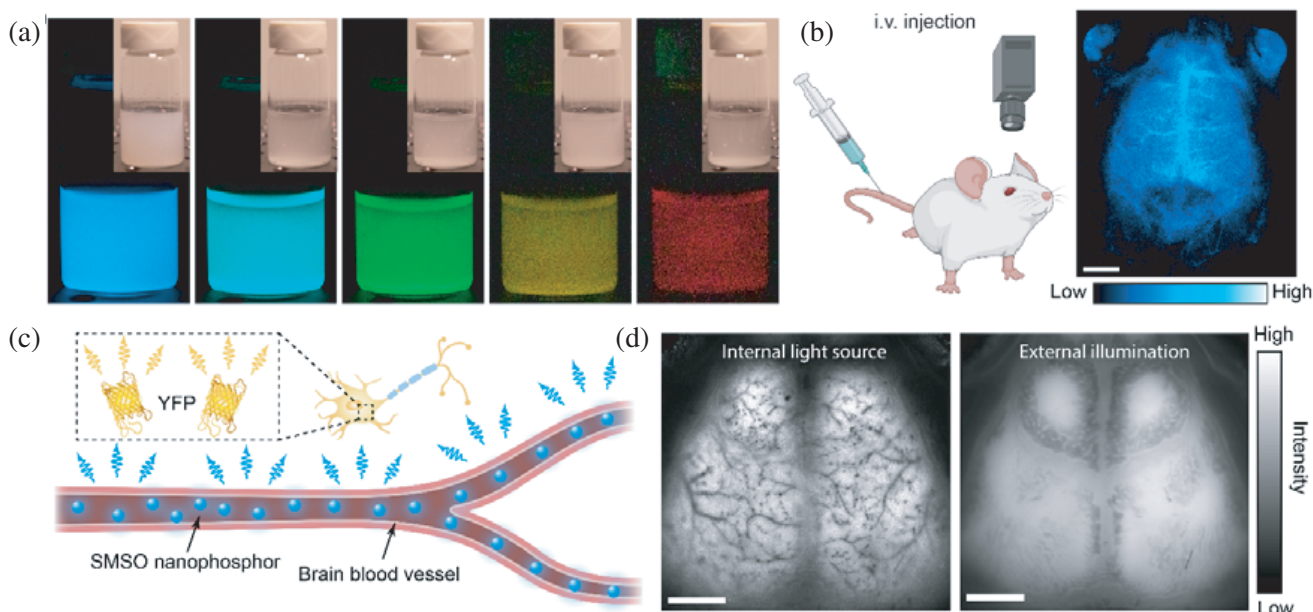


Figure 4. Multicolor internal light sources enabled by PerL nanomaterials. (a) PerL and the corresponding brightfield (insets) images of multicolor PerL nanomaterials suspended in an aqueous solution. (b) Left: Schematic showing the intravenous (i.v.) injection of PerL nanomaterials for brain imaging. Right: Transcranial PerL imaging of mouse brain vasculature. (c) Schematic showing the principle of PerL imaging of genetically encoded yellow fluorescent proteins (YFP) in the mouse brain. (d) YFP PerL (left) and fluorescence (right) images of the same mouse brain excited by a systemically delivered internal light source (left) and a conventional external light source (right). The scale bars represent 2.5 mm in (b) and 2 mm in (d), respectively. Adapted with Permission from [10]. Copyright 2022 American Association for the Advancement of Science.

the skull features (Figure 4(d)) [10]. Additionally, since no external stimuli is needed to activate PerL, this internal light source has no limitation on the penetration depth in theory. Furthermore, another unique advantage offered by PerL-based internal light sources is the large illumination volume, since the endogenous circulatory system covers the entire body. This advantage cannot be achieved with other existing *in vivo* light delivery techniques, as an external light source has limitations on the z -axis, while an implanted light source usually only illuminates a small volume of tissue.

4. OUTLOOK AND CONCLUSIONS

The widespread applications of light in biology have motivated innovations in light delivery methods, with recent demonstrations of novel internal light sources based on nanomaterials with ML and PerL. Although the utilities of these systemically delivered nanoscopic light sources have been demonstrated in non-invasive neuromodulation and transcranial brain imaging, their emerging applications in biology remain largely unexplored. In this section, we provide an outlook of a few potential directions where the internal light sources may enable new modalities in biology.

One interesting application of the FUS-mediated light source in neuroscience is the optogenetic screening of multiple brain regions. Specifically, once ML nanomaterials are delivered into the blood stream, the stimulation site can be easily shifted by changing the FUS focus, thus allowing the screening of the contributions from different brain regions to a certain behavior, such as addiction [44]. Furthermore, another unique application of PerL-based light sources in neuroscience is simultaneous neural activation across multiple brain regions or even throughout the entire brain. A previous study has validated the theoretical feasibility of activating stable step-function opsins (SSFO) using circulation delivered PerL nanoparticles [10]. Its experimental validation will offer a nice alternative to chemogenetics in non-invasive neuromodulation with a much shorter response time. Both above applications are challenging for implanted light sources, which have limited relocation ability and confined illumination volume.

Apart from neuroscience, internal light sources also have great application potentials in controlling gene-editing processes *in vivo*. There have been many demonstrations of light-activable gene-editing tools such as psCas9 and PA-Cre [26, 27, 45], and yet their *in vivo* applications are hindered by the lack of efficient and non-invasive light delivery methods in the deep tissue. The ML and PerL-based internal light sources may provide a solution to this problem, thus allowing organ-specific gene-editing with high temporal resolution *in vivo*. One potential challenge for this application is that the activation of gene-editing tools usually requires prolonged illumination. This challenge may be mitigated by applying an external excitation light to constantly recharge the PerL and ML nanomaterials when they pass through the superficial blood vessels.

Additionally, the continuous light emission from PerL nanomaterials may serve as an internal excitation light source for functional fluorescent proteins imaging to study the dynamics of biological processes. Although the emission intensity from PerL nanomaterials usually gradually decreases upon the cease of photoexcitation, a recent study has demonstrated that a remote periodic recharging light far from the imaging site can bring up the PerL intensity by leveraging the endogenous circulatory system [10]. We thus envision that constant remote recharging may keep the PerL intensity at a relatively stable level near the region of interest once the system has reached a steady state. This remote recharging method, combined with a dual channel collection system for correcting PerL intensity fluctuation [10], should enable PerL-excited real-time imaging of fluorescent proteins such as GCaMP in live animals [46].

In conclusion, the recent demonstrations of ML and PerL-based internal light sources have provided many new opportunities for using light to study biology. Compared with existing *in vivo* light delivery methods, this new modality allows deep-tissue (> 1 cm) light delivery in a non-invasive manner. Beyond preliminary demonstrations of non-invasive optogenetics and brain imaging, these systemically delivered nanoscopic light sources can also be applied to other biological systems, such as light-controlled gene-editing. Although existing demonstrations of these internal light sources have been limited to rodents, which have small organ sizes, we envision that they also have great application potential in humans with larger organs, as their penetration depth can readily reach the level of 10 cm due to the use of tissue-penetrant ultrasound and the endogenous circulatory system that covers the entire body [47].

Further improvement of the system can be achieved through the optimization of circulation lifetime and enhancement of the luminescence intensity [48]. With the rapid growth of ML and PerL nanomaterials toolbox, we envision that these systemically delivered nanoscopic light sources will eventually expand the utilities of light in biology.

ACKNOWLEDGMENT

X. W. acknowledges support from the Stanford Graduate Fellowship. S. C. acknowledges support from the Stanford Bio-X Bowes Graduate Fellowship and the NeuroTech training program supported by the National Science Foundation under Grant No. 1828993. G. H. acknowledges three awards by NIH (5R00AG056636-04, 1R34NS127103-01, and R01NS126076-01), a National Science Foundation (NSF) CAREER Award (2045120), an NSF EAGER Award (2217582), a Rita Allen Foundation Scholars Award, a Beckman Technology Development Grant, a grant from the focused ultrasound (FUS) Foundation, a gift from the Spinal Muscular Atrophy (SMA) Foundation, a gift from the Pinetops Foundation, two seed grants from the Wu Tsai Neurosciences Institute, and two seed grants from the Bio-X Initiative of Stanford University. Some schematics were created with BioRender.com.

REFERENCES

1. Hong, G., A. L. Antaris, and H. Dai, “Near-infrared fluorophores for biomedical imaging,” *Nat. Biomed. Eng.*, Vol. 1, 0010, Jan. 2017.
2. Zhang, F., V. Gradinaru, A. R. Adamantidis, et al., “Optogenetic interrogation of neural circuits: Technology for probing mammalian brain structures,” *Nat. Protoc.*, Vol. 5, No. 3, 439–456, Mar. 2010.
3. Yun, S. H. and S. J. J. Kwok, “Light in diagnosis, therapy and surgery,” *Nat. Biomed. Eng.*, Vol. 1, 0008, 2017.
4. Jiang, S., X. Wu, N. J. Rommelfanger, et al., “Shedding light on neurons: Optical approaches for neuromodulation,” *Natl. Sci. Rev.*, Vol. 9, nwac007, Jan. 18, 2022.
5. Kim, T.-I., J. G. McCall, Y. H. Jung, et al., “Injectable, cellular-scale optoelectronics with applications for wireless optogenetics,” *Science*, Vol. 340, No. 6129, 211–216, 2013.
6. Chen, S., A. Z. Weitemier, X. Zeng, et al., “Near-infrared deep brain stimulation via upconversion nanoparticle-mediated optogenetics,” *Science*, Vol. 359, No. 6376, 679–684, Feb. 9, 2018.
7. Montgomery, K. L., A. J. Yeh, J. S. Ho, et al., “Wirelessly powered, fully internal optogenetics for brain, spinal and peripheral circuits in mice,” *Nat. Methods*, Vol. 12, No. 10, 969–974, Oct. 2015.
8. Ruan, H., J. Brake, J. E. Robinson, et al., “Deep tissue optical focusing and optogenetic modulation with time-reversed ultrasonically encoded light,” *Sci. Adv.*, Vol. 3, No. 12, eaao5520, Dec. 2017.
9. Wu, X., X. Zhu, P. Chong, et al., “Sono-optogenetics facilitated by a circulation-delivered rechargeable light source for minimally invasive optogenetics,” *Proc. Natl. Acad. Sci. USA*, Vol. 116, No. 52, 26332–26342, Dec. 6, 2019.
10. Yang, F., X. Wu, H. Cui, et al., “A biomineral-inspired approach of synthesizing colloidal persistent phosphors as a multicolor, intravital light source,” *Sci. Adv.*, Vol. 8, No. 30, eabo6743, Jul. 29, 2022.
11. Yang, F., X. Wu, H. Cui, et al., “Palette of rechargeable mechanoluminescent fluids produced by a biomineral-inspired suppressed dissolution approach,” *J. Am. Chem. Soc.*, Vol. 144, No. 40, 18406–18418, Oct. 12, 2022.
12. Wang, W., X. Wu, K. W. Kevin Tang, et al., “Ultrasound-triggered in situ photon emission for noninvasive optogenetics,” *J. Am. Chem. Soc.*, Vol. 145, No. 2, 1097–1107, Jan. 18, 2023.
13. Yang, F., S. J. Kim, X. Wu, et al., “Principles and applications of sono-optogenetics,” *Adv. Drug Deliv. Rev.*, Vol. 194, 114711, Jan. 25, 2023.
14. Zhang, J. C., X. S. Wang, G. Marriott, et al., “Trap-controlled mechanoluminescent materials,” *Prog. Mater. Sci.*, Vol. 103, 678–742, Jun. 2019.
15. Zhuang, Y. and R. J. Xie, “Mechanoluminescence rebrightening the prospects of stress sensing: A review,” *Adv. Mater.*, Vol. 33, No. 50, e2005925, Dec. 2021.

16. Li, Y., M. Gecevicius, and J. Qiu, "Long persistent phosphors — From fundamentals to applications," *Chem. Soc. Rev.*, Vol. 45, No. 8, 2090–2136, Apr. 21, 2016.
17. Huang, K., N. Le, J. S. Wang, et al., "Designing next generation of persistent luminescence: Recent advances in uniform persistent luminescence nanoparticles," *Adv. Mater.*, Vol. 34, No. 14, e2107962, Apr. 2022.
18. Yang, F., H. Cui, X. Wu, et al., "Ultrasound-activated luminescence with color tunability enabled by mechanoluminescent colloids and perovskite quantum dots," *Nanoscale*, Vol. 15, No. 4, 1629–1636, Jan. 27, 2023.
19. Maldiney, T., A. Bessiere, J. Seguin, et al., "The in vivo activation of persistent nanophosphors for optical imaging of vascularization, tumours and grafted cells," *Nat. Mater.*, Vol. 13, No. 4, 418–426, Apr. 2014.
20. Li, Z., Y. Zhang, X. Wu, et al., "Direct aqueous-phase synthesis of sub-10 nm "luminous pearls" with enhanced in vivo renewable near-infrared persistent luminescence," *J. Am. Chem. Soc.*, Vol. 137, No. 16, 5304–5307, Apr. 29, 2015.
21. Pei, P., Y. Chen, C. Sun, et al., "X-ray-activated persistent luminescence nanomaterials for NIR-II imaging," *Nat. Nanotechnol.*, Vol. 16, No. 9, 1011–1018, Sep. 2021.
22. Miao, Q., C. Xie, X. Zhen, et al., "Molecular afterglow imaging with bright, biodegradable polymer nanoparticles," *Nat. Biotechnol.*, Vol. 35, No. 11, 1102–1110, Nov. 2017.
23. Wu, X., Y. Jiang, N. J. Rommelfanger, et al., "Tether-free photothermal deep-brain stimulation in freely behaving mice via wide-field illumination in the near-infrared-II window," *Nat. Biomed. Eng.*, Vol. 6, No. 6, 754–770, Jun. 2022.
24. Day, R. N. and M. W. Davidson, "The fluorescent protein palette: Tools for cellular imaging," *Chem. Soc. Rev.*, Vol. 38, No. 10, 2887–2921, Oct. 2009.
25. Fenno, L., O. Yizhar, and K. Deisseroth, "The development and application of optogenetics," *Annu. Rev. Neurosci.*, Vol. 34, 389–412, 2011.
26. Zhou, X. X., X. Zou, H. K. Chung, et al., "A single-chain photoswitchable CRISPR-Cas9 architecture for light-inducible gene editing and transcription," *ACS Chem. Biol.*, Vol. 13, No. 2, 443–448, Feb. 16, 2018.
27. Nihongaki, Y., F. Kawano, T. Nakajima, et al., "Photoactivatable CRISPR-Cas9 for optogenetic genome editing," *Nat. Biotechnol.*, Vol. 33, No. 7, 755–760, Jul. 2015.
28. Su, X. L., X. Y. Kong, K. S. Sun, et al., "Enhanced blue afterglow through molecular fusion for bio-applications," *Angew. Chem. Int. Edit.*, Vol. 61, e202201630, Jul. 4, 2022.
29. Lawson, N. D. and B. M. Weinstein, "In vivo imaging of embryonic vascular development using transgenic zebrafish," *Dev. Biol.*, Vol. 248, No. 2, 307–318, Aug. 15, 2002.
30. Kim, T. H. and M. J. Schnitzer, "Fluorescence imaging of large-scale neural ensemble dynamics," *Cell*, Vol. 185, No. 1, 9–41, Jan. 6, 2022.
31. Kim, S., T. Kyung, J. H. Chung, et al., "Non-invasive optical control of endogenous Ca(2+) channels in awake mice," *Nat. Commun.*, Vol. 11, 210, Jan. 10, 2020.
32. Xu, X., H. Liu, and L. V. Wang, "Time-reversed ultrasonically encoded optical focusing into scattering media," *Nat. Photonics*, Vol. 5, No. 3, 154–157, Mar. 2011.
33. Hampson, K. M., R. Turcotte, D. T. Miller, et al., "Adaptive optics for high-resolution imaging," *Nat. Rev. Methods Primers*, Vol. 1, 68, 2021.
34. Streich, L., J. C. Boffi, L. Wang, et al., "High-resolution structural and functional deep brain imaging using adaptive optics three-photon microscopy," *Nat. Methods*, Vol. 18, No. 10, 1253–1258, Oct. 2021.
35. Canales, A., S. Park, A. Kiliyas, et al., "Multifunctional fibers as tools for neuroscience and neuroengineering," *Acc. Chem. Res.*, Vol. 51, No. 4, 829–838, Apr. 17, 2018.
36. Park, S. I., D. S. Brenner, G. Shin, et al., "Soft, stretchable, fully implantable miniaturized optoelectronic systems for wireless optogenetics," *Nat. Biotechnol.*, Vol. 33, No. 12, 1280–1286, Dec. 2015.

37. Gunaydin, L. A., L. Grosenick, J. C. Finkelstein, et al., “Natural neural projection dynamics underlying social behavior,” *Cell*, Vol. 157, No. 7, 1535–1551, Jun. 19, 2014.
38. Salatino, J. W., K. A. Ludwig, T. D. Y. Kozai, et al., “Glial responses to implanted electrodes in the brain,” *Nat. Biomed. Eng.*, Vol. 1, No. 11, 862–877, Nov. 2017.
39. Chen, Y., N. J. Rommelfanger, A. I. Mahdi, et al., “Low is flexible electronics advancing neuroscience research?,” *Biomaterials*, Vol. 268, 120559, Jan. 2021.
40. Miyazaki, T., S. Chowdhury, T. Yamashita, et al., “Large timescale interrogation of neuronal function by fiberless optogenetics using lanthanide micro-particles,” *Cell Rep.*, Vol. 26, No. 4, 1033–1043, Jan. 22, 2019.
41. Pisanello, F., G. Mandelbaum, M. Pisanello, et al., “Dynamic illumination of spatially restricted or large brain volumes via a single tapered optical fiber,” *Nat. Neurosci.*, Vol. 20, No. 8, 1180–1188, Aug. 2017.
42. Mohanty, A., Q. Li, M. A. Tadayon, et al., “Reconfigurable nanophotonic silicon probes for sub-millisecond deep-brain optical stimulation,” *Nat. Biomed. Eng.*, Vol. 4, No. 2, 223–231, Feb. 2020.
43. Speed, C. A., “Therapeutic ultrasound in soft tissue lesions,” *Rheumatology*, Vol. 40, No. 12, 1331–1336, Dec. 2001.
44. Pascoli, V., M. Turiault, and C. Luscher, “Reversal of cocaine-evoked synaptic potentiation resets drug-induced adaptive behaviour,” *Nature*, Vol. 481, No. 7379, 71–75, Dec. 7, 2011.
45. Morikawa, K., K. Furuhashi, C. de Sena-Tomas, et al., “Photoactivatable Cre recombinase 3.0 for in vivo mouse applications,” *Nat. Commun.*, Vol. 11, 2141, May 1, 2020.
46. Lin, M. Z. and M. J. Schnitzer, “Genetically encoded indicators of neuronal activity,” *Nat. Neurosci.*, Vol. 19, No. 9, 1142–1153, Aug. 26, 2016.
47. Alter, K. E. and B. I. Karp, “Ultrasound guidance for botulinum neurotoxin chemodenervation procedures,” *Toxins*, Vol. 10, No. 1, Dec. 28, 2017.
48. Zhong, Y., Z. Ma, F. Wang, et al., “In vivo molecular imaging for immunotherapy using ultra-bright near-infrared-IIb rare-earth nanoparticles,” *Nat. Biotechnol.*, Vol. 37, No. 11, 1322–1331, Nov. 2019.